

Article

Using Object-Oriented Classification for Coastal Management in the East Central Coast of Florida: A Quantitative Comparison between UAV, Satellite, and Aerial Data

Bo Yang ^{1,*} , Timothy L. Hawthorne ¹, Hannah Torres ² and Michael Feinman ¹

¹ Department of Sociology, University of Central Florida, Orlando, FL 32816, USA

² Department of Political Science and Geography, Old Dominion University, Norfolk, VA 23529, USA

* Correspondence: Bo.Yang@ucf.edu

Received: 1 July 2019; Accepted: 25 July 2019; Published: 27 July 2019



Abstract: High resolution mapping of coastal habitats is invaluable for resource inventory, change detection, and inventory of aquaculture applications. However, coastal areas, especially the interior of mangroves, are often difficult to access. An Unmanned Aerial Vehicle (UAV), equipped with a multispectral sensor, affords an opportunity to improve upon satellite imagery for coastal management because of the very high spatial resolution, multispectral capability, and opportunity to collect real-time observations. Despite the recent and rapid development of UAV mapping applications, few articles have quantitatively compared how much improvement there is of UAV multispectral mapping methods compared to more conventional remote sensing data such as satellite imagery. The objective of this paper is to quantitatively demonstrate the improvements of a multispectral UAV mapping technique for higher resolution images used for advanced mapping and assessing coastal land cover. We performed multispectral UAV mapping fieldwork trials over Indian River Lagoon along the central Atlantic coast of Florida. Ground Control Points (GCPs) were collected to generate a rigorous geo-referenced dataset of UAV imagery and support comparison to geo-referenced satellite and aerial imagery. Multi-spectral satellite imagery (Sentinel-2) was also acquired to map land cover for the same region. NDVI and object-oriented classification methods were used for comparison between UAV and satellite mapping capabilities. Compared with aerial images acquired from Florida Department of Environmental Protection, the UAV multi-spectral mapping method used in this study provided advanced information of the physical conditions of the study area, an improved land feature delineation, and a significantly better mapping product than satellite imagery with coarser resolution. The study demonstrates a replicable UAV multi-spectral mapping method useful for study sites that lack high quality data.

Keywords: coastal management; multi-spectral drone mapping; NDVI; object-oriented classification; Sentinel-2

1. Introduction

High quality mapping of land cover is invaluable for analysis applications such as resource inventories, change detection, and inventories of aquaculture. However, coastal vegetation ecosystems, especially the interior of mangrove forests, are often difficult to access. To overcome this challenge, many researchers use remote sensing technology to monitor and analyze coastal ecosystems [1,2]. Satellite remote sensing data, e.g., Sentinel series, can provide multi-spectral and historical observations, but due to relatively low spatial resolution, mangroves are difficult to distinguish from adjacent thorn

scrubs from satellite sensors [2,3]. In such cases, high quality data with finer resolution collected from multi-spectral imagery can be a more appropriate option for land cover monitoring for coastal areas.

A typical satellite remote sensing system, such as Landsat 8 OLI/TIRS, ASTER, and Sentinel-2, has a relatively coarse resolution of 10 to 30 m [4,5], while image sensors mounted on unmanned aerial vehicles (UAVs) can provide images with a finer resolution (sub-meter) and more spatially accurate information [6]. Acquiring data with UAV approaches is also often less expensive and more convenient than hiring out manned aircrafts, especially in more remote and inaccessible places. In addition, although satellites capture images of remote areas and difficult terrain, they often have infrequent and inflexible temporal revisit cycles. UAVs, on the other hand, can collect on-demand data. A typical UAV/drone mapping project will involve multiple stakeholders (e.g. scientists, engineers, pilots), technologies (e.g. drone platforms, controllers, software packages, sensors), parameters (e.g. flight altitude, scientific sensor calibration date and processes, scientific parameters, FAA airspace regulations), and complex processes (e.g. data stitching, data management, data pre- and post-processing), many of which can influence the utilization and interpretation of the data [7]. In order to fly drones under the FAA's Small UAS Rule (Part 107) for research purposes, remote pilots must obtain a certificate from the FAA. There is also background knowledge needed for pre- and post-processing of the drone mapping products, such as image stitching and geo-referencing.

Multi-spectral mapping facilitates coastal land cover analysis because vegetation can be extracted semi-automatically via image classification techniques. The living green plants have a higher DN value in near infrared (NIR) bands, thus satellite remote sensing with multi-spectral sensors have been widely used for coastal land cover analysis [8]. Earlier research using UAV mapping for land cover was limited by its stock camera which lacked a multi-spectral sensor [9–11]. Despite using high-resolution UAV imagery, vegetation analysis results are usually no better than the multi-spectral mapping with coarse spatial resolution.

UAV technology has been developing rapidly. A variety of sensors onboard UAV platforms have been implemented and there have been many research projects employing UAVs to collect hyperspectral [12–14] and thermal data [15,16]. Some researchers also used LiDAR sensors mounted on UAV platforms to collect elevation data and develop DEMs [17–19]. With advances in multi-spectral mapping sensors, UAV mapping can achieve the same spectral resolution but much higher spatial resolution compared with satellite mapping. Although it is well known that UAV mapping provides better land cover analysis resulting from its high resolution [3,14,20], few studies have made both qualitative and quantitative comparisons between UAV mapping methods with conventional remote sensing datasets, such as satellite imagery and aerial imagery.

In this research, we utilized two types of UAV techniques—traditional three bands and multi-spectral—to collect images at a higher spatial resolution than those provided by satellite sensors for a portion of the Indian River Lagoon along the central Atlantic coast of Florida. Additionally, ground control points (GCPs) were collected in the study area to rectify and geo-reference the UAV imagery as well as to register remote sensing data. The objective of this study is to compare the qualitative and quantitative improvements of multi-spectral UAV sensors compared to multi-spectral satellite sensors. We calculated the normalized difference vegetation index (NDVI) to illustrate that more spatial information about vegetation can be extracted from multi-spectral UAV mapping than from satellite imagery. In comparison with coarse resolution satellite imagery, the UAV mapping method used in this study provided advanced information about the physical conditions of the study area, an improved land feature delineation, and a more comprehensive understanding of the conditions of the vegetation. Another main objective of the study was to examine the improvements that finer resolution data would facilitate for a more comprehensive land cover analysis in the study area. An object-oriented classification method was used to classify land cover for UAV and satellite mapping products, respectively. Quantitatively, both UAV and satellite mapping classification results were compared with aerial imagery acquired by the Florida Department of Environmental Protection.

2. Study Area

This study focused on River Breeze Park in Oak Hill, located along the Indian River Lagoon (IRL) on Florida's Atlantic coast (Figure 1). The Indian River Lagoon is an estuary comprising three smaller water bodies: Mosquito Lagoon, Banana River, and Indian River. Oak Hill sits on Mosquito Lagoon in the northernmost part of the IRL, in an area known as Florida's Space Coast. The IRL system is one of the most biodiverse estuaries in the Northern Hemisphere and is home to more than 4,300 species of plants and animals (<https://fau.edu/hboi/irlo>). Because of its ecological importance and degradation due to human activity, the Indian River Lagoon was named an "Estuary of National Significance" in 1990, becoming part of the United States National Estuary Program (<https://fau.edu/hboi/irlo>). The study region of IRL is a typical natural marsh consisting of red mangroves (*Rhizophora mangle*) or cordgrass (*Spartina alterniflora*) at the water's edge with flat high marsh areas of herbaceous halophytes, such as *Batis maritima*, *Salicornia virginica*, and *Salicornia bigelovii*, mixed with scattered black mangroves (*Avicennia germinas*) further inland [21].

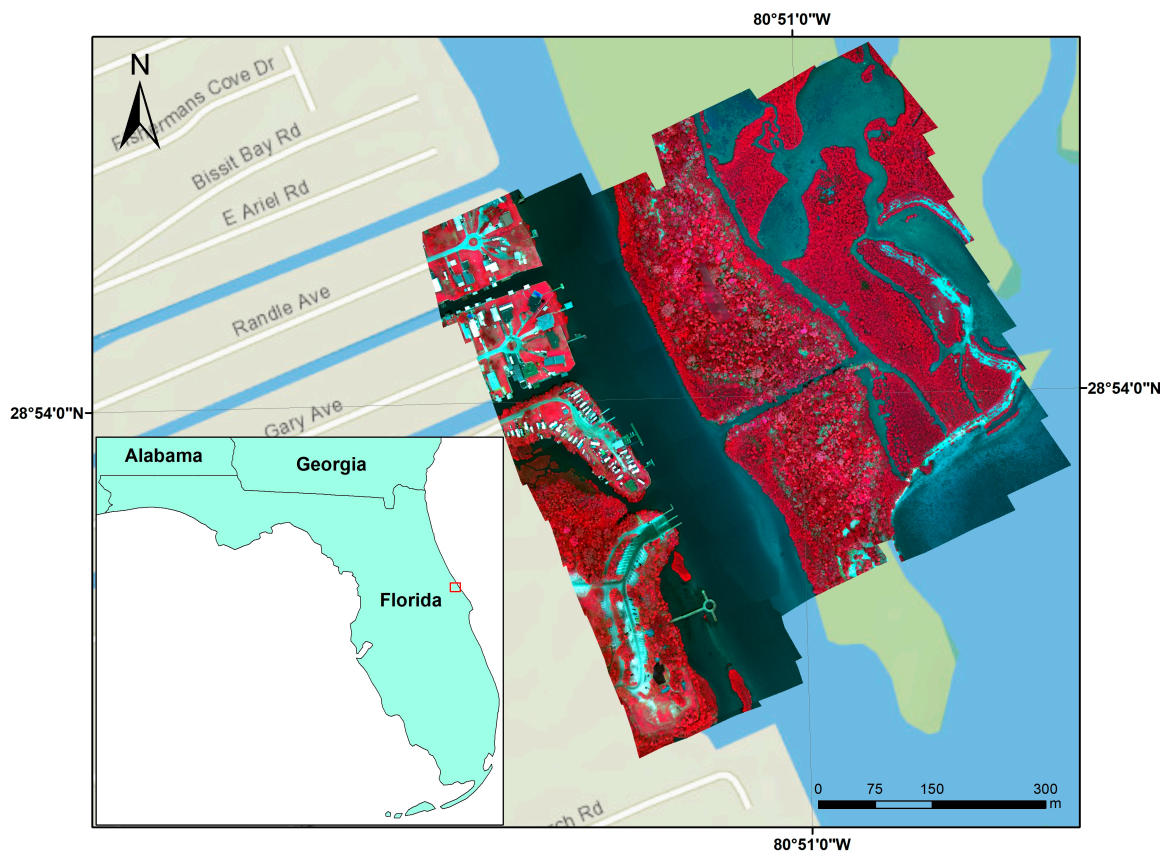


Figure 1. Multi-spectral drone mapping area in Oak Hill along Mosquito Lagoon along Florida's central Atlantic coast.

Mangroves are an important component of coastal ecosystems, yet the IRL has seen a devastating loss in mangroves over time. In the IRL, between the 1940s and 2013, 85% of mangroves were removed for housing and development [22]. In 2019, lagoon health is better near ocean inlets, and pollution is worse in areas away from inlets, such as Mosquito Lagoon, North IRL, and the Banana River.

3. Data and Methods

3.1. Data

3.1.1. UAV Data Acquisition

In this study, we used two UAVs: A Parrot Bluegrass quadcopter with a Parrot Sequoia+ multispectral sensor (Figure 2a); the sensor has four separated bands including, Green (550 nm), Red (660 nm), Red Edge (735 nm), and Near infrared (790 nm), and a DJI Phantom 4 Pro quadcopter (Figure 2b) equipped with a stock 1/2.3 inch (1.10 cm) RGB CMOS camera sensor with 12.4 m effective pixels (DJI.com) [23,24].



Figure 2. (a) Parrot Bluegrass quadcopter with Parrot Sequoia sensor; (b) DJI Phantom 4 Pro quadcopter with stock RGB camera.

A series of UAV flights over the study area were conducted on 31 October 2018, 28 February, 5 March, and 9 May 2019. Data acquired on 5 March have the best image quality; imagery for the other dates were used as ancillary data to fill data gaps. Flights were scheduled on clear days with good visibility and relatively low wind speed. Both UAV systems were set to fly at a height of 120 m (400 ft), achieving an ideal balance between image coverage and spatial resolution, while adhering to US Federal Aviation Administration (FAA) Part 107 flight guidelines. Figure 3 shows the flight plans for both UAV mapping systems. The flight path was pre-defined to evenly cover the study area and overlapping area between adjacent images was set with 70/60 frontlap/sidelap to achieve the best image stitching quality. In this study, we focused on the Parrot Bluegrass multi-spectral imagery to perform the analyses because it has additional near infrared (NIR) and red edge bands. The NIR bands are very responsive to vegetation compared to the other visible bands. The normal red, green, blue (RGB) imagery taken by the DJI Phantom 4 Pro was used as auxiliary data to support the collection of multi-spectral imagery and help to identify ground control points. As shown in Figure 2, 76 images were taken during each flight and then stitched and geo-referenced to a multi-spectral orthomosaic image covering the study area.

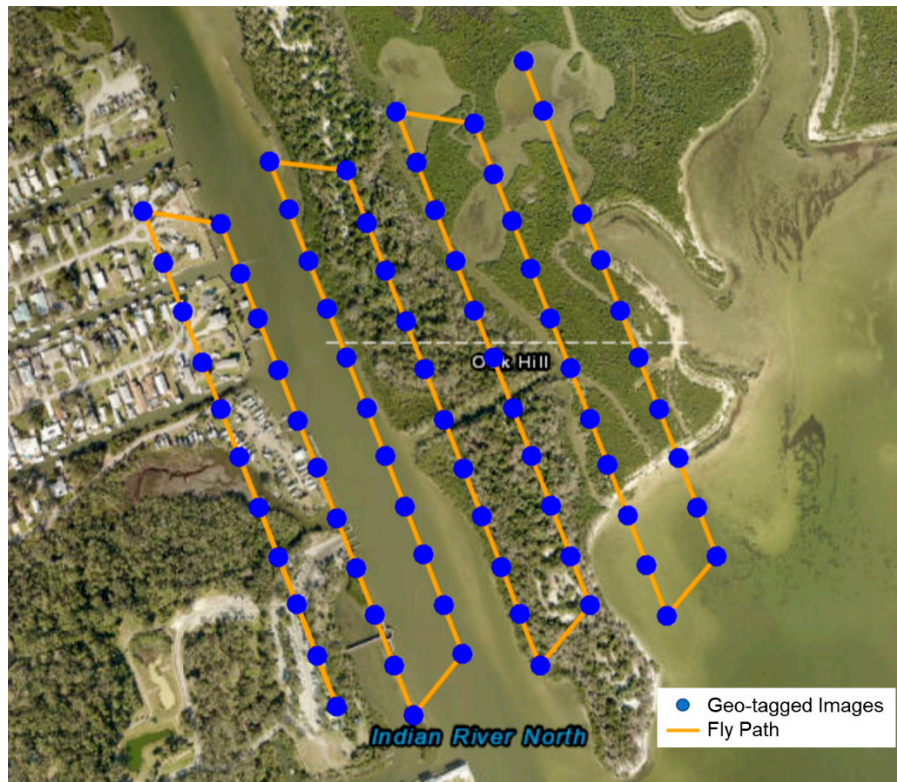


Figure 3. UAV flight plan over the River Breeze with image capture locations and flight path.

3.1.2. Satellite and Aerial Remote Sensing Data

The Sentinel-2 series (European Space Agency) is a relatively new satellite remote sensing system comprised of two identical satellites with high spatial resolution (NIR and RGB bands in 10–20 m). The Multi-Spectral Instrument (MSI) onboard these satellites acquires images in 13 spectral bands spanning from 400 nm to 2400 nm [25]. Because it is a relatively new satellite platform with high spatial, temporal, radiometric resolution, high signal-to-noise ratio (SNR), and wide field of view, Sentinel-2 is a significantly better platform than the more commonly used Landsat series for coastal monitoring and hydrological modelling [26,27].

We acquired data for the study region sourced from the Sentinel-2 on Amazon Web Services (AWS), which is a combined level 1 product from March 2019 (Figure 4a). Four bands, all of which have a spatial resolution of 10 m, were used—NIR, Red, Green, and Blue. Figure 4 shows the NIR false color combination of the Sentinel-2 satellite remote sensing imagery. We used the NIR band as a red channel of the combination, red band as green, green band as blue, thus the vegetation coverage could be highlighted in red tones. Compared with Landsat satellite imagery, Sentinel-2 provides higher spatial resolution (10 m) and higher radiometric resolution (12-bit). Satellite remote sensing techniques are able to provide frequent observations of the lagoon for those regions difficult to reach by humans, but these techniques suffer from lower spatial resolution limiting the fine scale classification and vegetation detection necessary to understand the coastal ecosystem. Aerial photography, on the other hand, provides a very fine spatial resolution. Florida Aerial Photography Archive Collection (APAC), Florida's largest collection of aerial photography, has collected over 450,000 digital images that date back to 1951. The most recent aerial survey was completed in 2015. In addition to APAC imagery, our team utilized UAV mapping in the study site to offer a well-balanced solution for coastal mapping, given its relatively inexpensive manipulation; imagery processing; and on-demand, high-resolution capability. Besides the satellite remote sensing imagery, we also acquired aerial photography collected by the Florida Department of Environmental Protection (FDEP, Figure 4b). FDEP collects aerial imagery

for the coastal areas of Florida every 3–5 years for coastal management and change detection. The aerial imagery from FDEP used in this study was captured and processed in 2015 at 0.25 m spatial resolution.

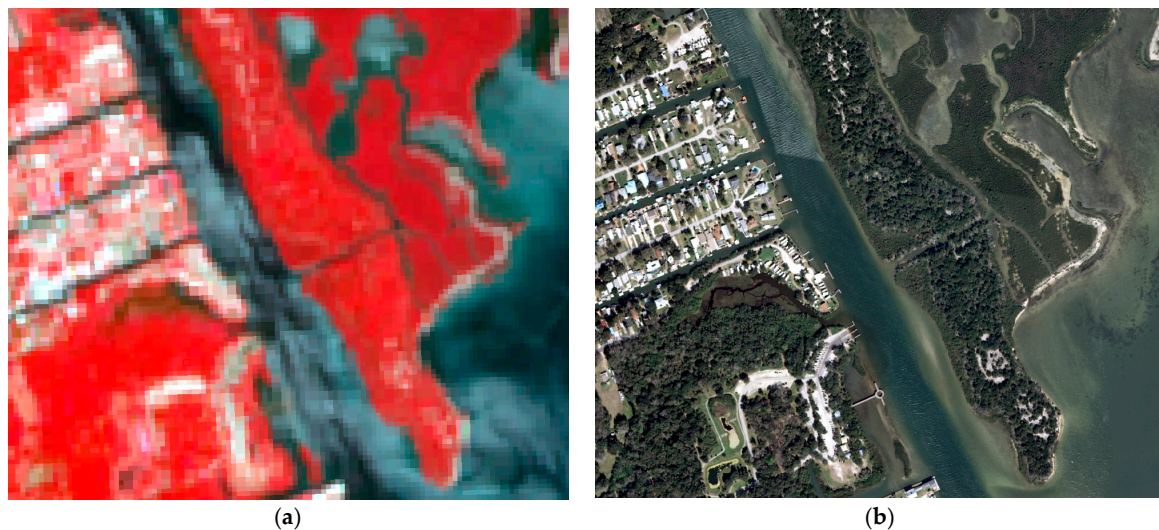


Figure 4. (a) Sentinel-2 near infrared false color combination; (b) aerial natural color imagery for the study area.

3.2. Methods

3.2.1. The Use of Vegetation Indices

NDVI is a well-established indicator for the presence and condition (abundance, vigor, and health) of vegetation [28]. It largely compensates for changing illumination conditions, surface slope, and viewing aspects and highlights vegetation condition. Mathematically, NDVI involves the calculation of the red band and near infrared band in multispectral imagery and has a numerical range of (−1.0, 1.0). The NDVI images are able to reflect short-term and long-term vegetation changes and land cover phenology over time [29]. Other popular indexes such as Global Environment Monitoring Index (GEMI) and the Angular Vegetation Index (AVI) were also developed to examine vegetational conditions, but NDVI is the most widely used index in the remote sensing field. The NDVI is calculated from band math of multi-spectral data as follows:

$$NDVI = \frac{NIR - RED}{NIR + RED}$$

Generally, if there is much more reflected radiation in near-infrared wavelengths than in visible wavelengths, the vegetation in that pixel is more likely to be dense and may contain some types of vegetation. For our multi-spectral UAV mapping, it is feasible to calculate the NDVI because the RED and NIR bands are included in the multi-spectral sensor on board the UAV system. It is also possible to calculate NDVI for Sentinel-2 by using band 8 (NIR) and band 4 (Red). In this study, we proposed a replicable UAV mapping method which is also capable of multi-spectral mapping and generating NDVI maps at much higher spatial resolution than satellite platforms.

3.2.2. Object-Oriented Classification Method

Object-oriented classification generates image objects, which are derived by dividing the whole image into small objects according to the shape, size, and spectral content of the image segments. Because object-oriented classification generates classes at the object level, with appropriate training samples and parameters, it has the capability to delineate objects at a local scale [30]. This characteristic can be particularly valuable in urban watershed studies where there are often multiple objects with complicated spatial distribution patterns. When compared to traditional pixel-based classification methods, which use regular pixels, object-oriented classification is more appropriate for hydrologic modeling and vegetation detection [31]. As a result, object-oriented imagery classification has been widely used for automatic and semi-automatic analyses [32–34].

In this research, we performed an object-oriented classification on both UAV and satellite multi-spectral data using eCognition (Trimble.com). To perform the object-oriented multi-resolution classification, we utilized four bands (red, green, Red Edge, NIR). Because the NIR band of Sentinel-2 is more responsive to vegetation, we assigned it a larger weight than the other bands to take advantage of its measurements.

The shape and size of the objects on the imagery are important parameters in the object-oriented classification. We identified the suitable size, which depicted optimal size for objects in the study area. We set object size to 200 pixels for the UAV imagery (Figure 5) and 10 pixels for the satellite imagery. To calibrate the classification parameters, a sample of classification results was compared to the aerial imagery. A new classification map was produced by adjusting the coefficients of the shape and compactness of the image objects to 0.1 and 0.5.

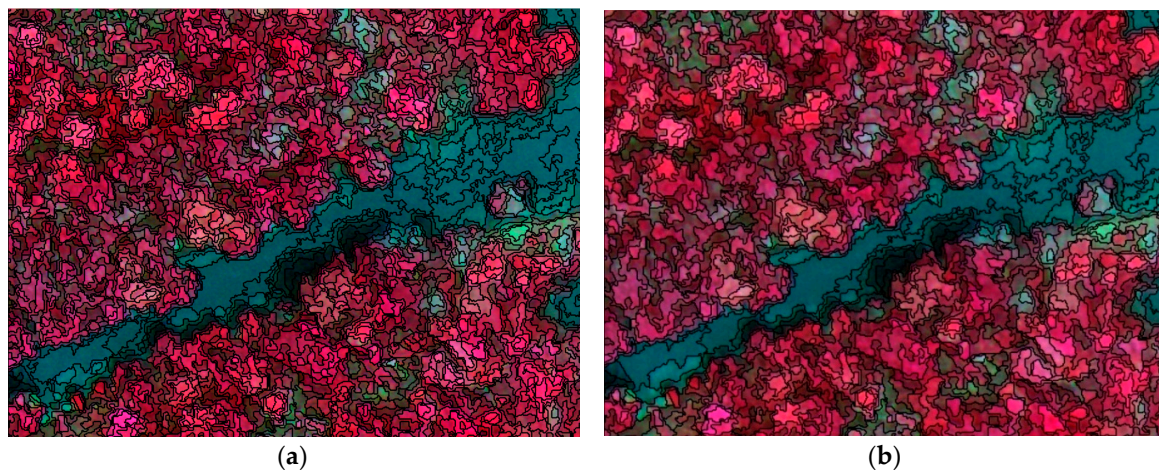


Figure 5. Object-oriented imagery segmentation for the UAV orthomosaic imagery, (a) object size 200; (b) object size 300.

The ground truth data were collected with the drone mapping fieldwork, including GPCs and in situ targets from high-performance GPS which were used as validation data for the object-oriented classification. We selected several ground-truth targets, such as mangroves, trees, buildings, and water bodies for training and validation of the remote sensing data (Figure 6). Those targets will be corresponded to the pixels/objects on the imagery; thus, those can be used to validate the classification results. As shown in Figure 6, we collected a polygon of the target for seven of the different classes. Ground-truth validation results show that different land features are well delineated in the classification map. As such, the object-oriented classification was deemed to have successfully classified each class, and the map was considered suitable for use in further analyses.

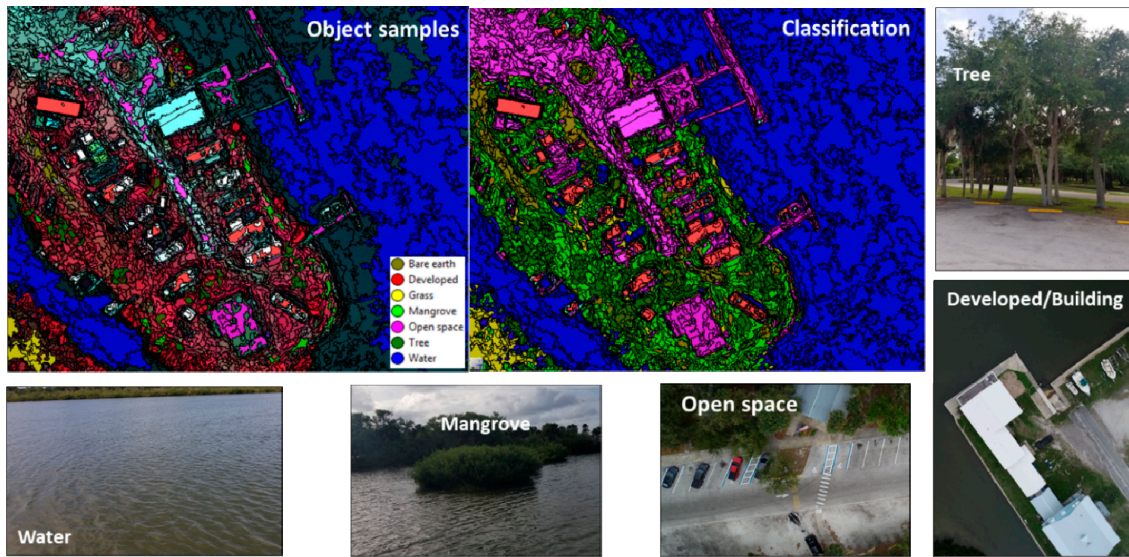


Figure 6. Selection of object training samples and ground truth validations.

4. Results

4.1. UAV Mapping Products and Calibration

The images captured by the multi-spectral camera on board the Parrot Bluegrass were stitched and processed into multi-spectral orthomosaic imagery via the Pix4D software. Meanwhile, the images collected by the DJI Phantom 4 Pro were processed using Drone2Map software as 2D and 3D products, including orthomosaic, Digital Surface Model (DSM), Digital Elevation Model (DEM), and point clouds. Pix4D and Drone2Map implement the same Structure from Motion-Multiview Stereo (SfM-MVS) photogrammetric techniques to tie multiple overlapping images together and generate the previously mentioned geospatial data products. Parrot multi-spectral orthomosaic imagery was compared with the satellite remote sensing data, while the RGB images from DJI Phantom 4 Pro were used as auxiliary data to help identify the GCPs.

Figure 7 shows the orthomosaic and geo-referenced UAV products for both multi-spectral imagery from the Parrot Bluegrass and nature color imagery from the DJI Phantom 4. To calibrate the data and rectify the UAV imagery, 11 GCPs were collected from easily discernable land features, such as docks, roads, and corners of parking lots (Figure 7). A Trimble R1 high-performance GNSS System was used to collect the GCPs around the study area, which delivers GNSS positions in real-time without the need for post-processing. The high-performance GPS has the capability of measuring and recording geographic coordinates with a horizontal error less than 0.5 m. For the region that is not accessible for the GCPs, we selected 11 more GCP points from the Google Earth aerial imagery, so that the GCP points were evenly distributed throughout the study area. By incorporating those GCP points, a high quality orthomosaic was generated from the UAV imagery.

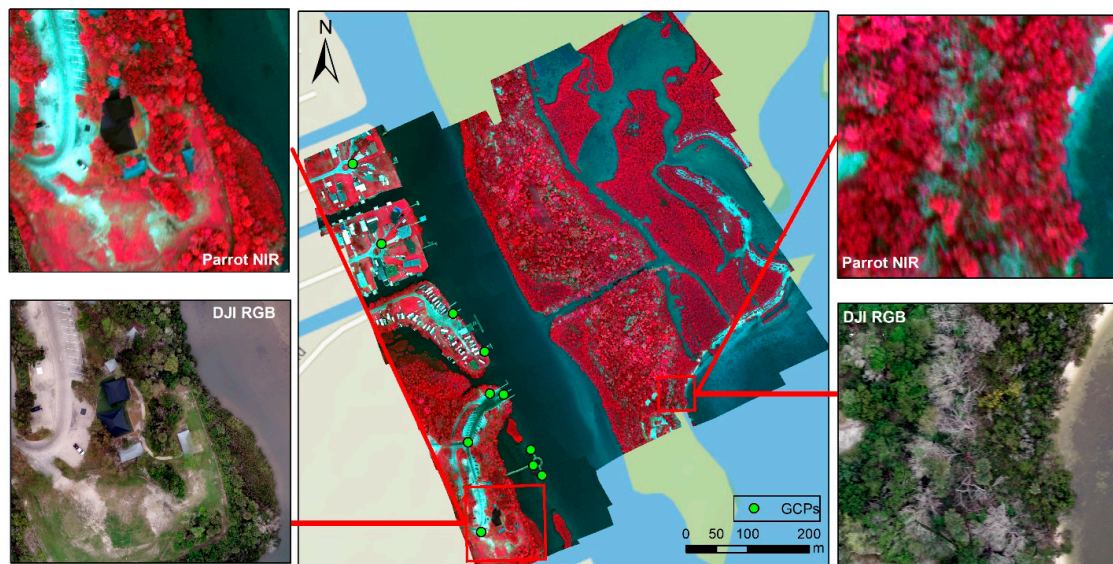


Figure 7. Orthomosaic and geo-referenced UAV products at 0.25 m spatial resolution using the near infrared false color combination. Two enlarged areas show both false color images from the Parrot Bluegrass and nature color image from the DJI Phantom 4 Pro.

4.2. NDVI Comparison between UAV and Satellite Mapping

First, we aimed to compare the data quality in terms of NDVI between UAV and satellite multi-spectral mapping products. Higher reflectance in the NIR band of the electromagnetic spectrum reflects a healthier vegetation in terms of a high NDVI value [2,35]. On the other hand, non-vegetated surfaces such as water bodies are represented as negative values in NDVI because of the electromagnetic absorption quality of water [1]. Based on Equation (1), NDVI maps from UAV and satellite multispectral mapping were generated, respectively.

Figure 8 shows the NDVI color map calculated from UAV and satellite multi-spectral mapping products. The areas containing a dense vegetation canopy include positive values from 0.3 to 0.8, while water bodies are characterized by negative values in this index. Both NDVI maps extract the water and vegetation coverage well. However, the high spatial resolution map created from UAV imagery affords much more information. As shown in Figure 8, the UAV mapping product clearly outperforms the satellite mapping in NDVI maps, offering a more detailed land pattern and more comprehensive vegetation information. Riparian features along the coastal area and roads and docks near the shore are well recognized in the image created from the multi-spectral UAV mapping. The different types of vegetation and bare earth can be distinguished in the UAV imagery. The denser and healthier vegetation inside the lagoon can be identified on the NDVI map. The dense vegetation has higher NDVI values around 0.7, while the sparse vegetation displays a lower NDVI value around 0.3 to 0.4. Bare earth and mud have very low NDVI values, close to zero. The histograms of the NDVI maps from UAV mapping and satellite remote sensing are also plotted in Figure 9. The left y-axis stands for the frequency of the UAV histogram, while the right y-axis stands for the frequency of the Sentinel-2 histogram. With the overlay of NDVI histograms from Sentinel and UAV, it is apparent that the variance and frequency of the UAV mapping histogram are much higher due to the finer spatial resolution. In addition, the NDVI histogram from the UAV mapping appeared much smoother and more informative on the UAV imagery compared to satellite imagery (Figure 9). The multi-Gaussian distribution reflects the different types of land cover captured by the UAV NDVI maps. Different components in the multi-Gaussian distribution stand for the different land covers with approximate mean values of water bodies (-0.51), developed areas (-0.28), and vegetation (0.41).

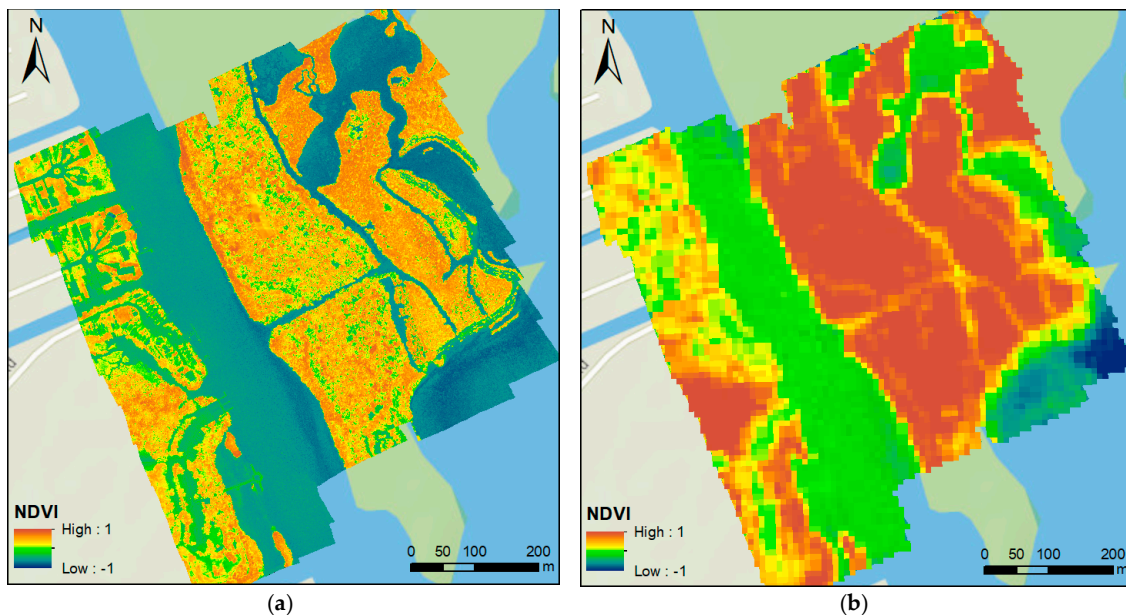


Figure 8. NDVI maps from: (a) UAV multi-spectral mapping; (b) Sentinel-2 satellite remote sensing.

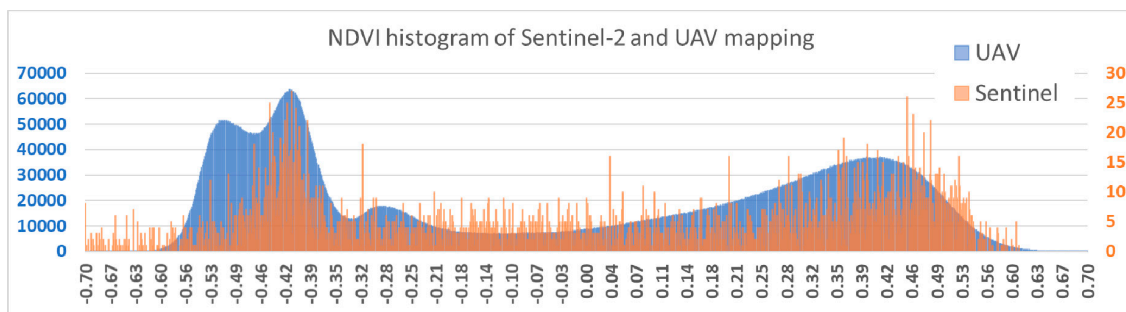


Figure 9. Histograms for NDVI map for UAV mapping and satellite remote sensing.

4.3. Comparison of Object-Oriented Classification Results

To illustrate the results of our analyses in more detail, object-oriented classifications on UAV mapping, satellite remote sensing, and aerial mapping are performed using eCognition (Trimble.com). We clipped the satellite and aerial mapping to a similar area to make a better visual comparison, as shown in Figure 10. Multi-resolution classification was used because the satellite imagery contains NIR, red edge, red, green, and blue bands; hence, the same classification was used on the UAV and aerial imagery. To obtain the best classification results, we set the object size to 200 for the UAV and aerial imagery, and 50 for satellite images. These sizes corresponded to the average number of pixels for objects in the study region. In order to compare the object-oriented classification method with the conventional pixel-based classification method, we also used the ISODATA unsupervised classification method on the UAV multi-spectral image [36]. The conventional pixel-based method generates results with more fragmentized classifications. There are some small pieces of developed areas in the water body due to the abnormal value of pixels. On the other hand, the object-oriented classification method is able to model the objects considering its spectral, shape, and relative locations, achieving more accurate results and better delineation of the objects' shape.

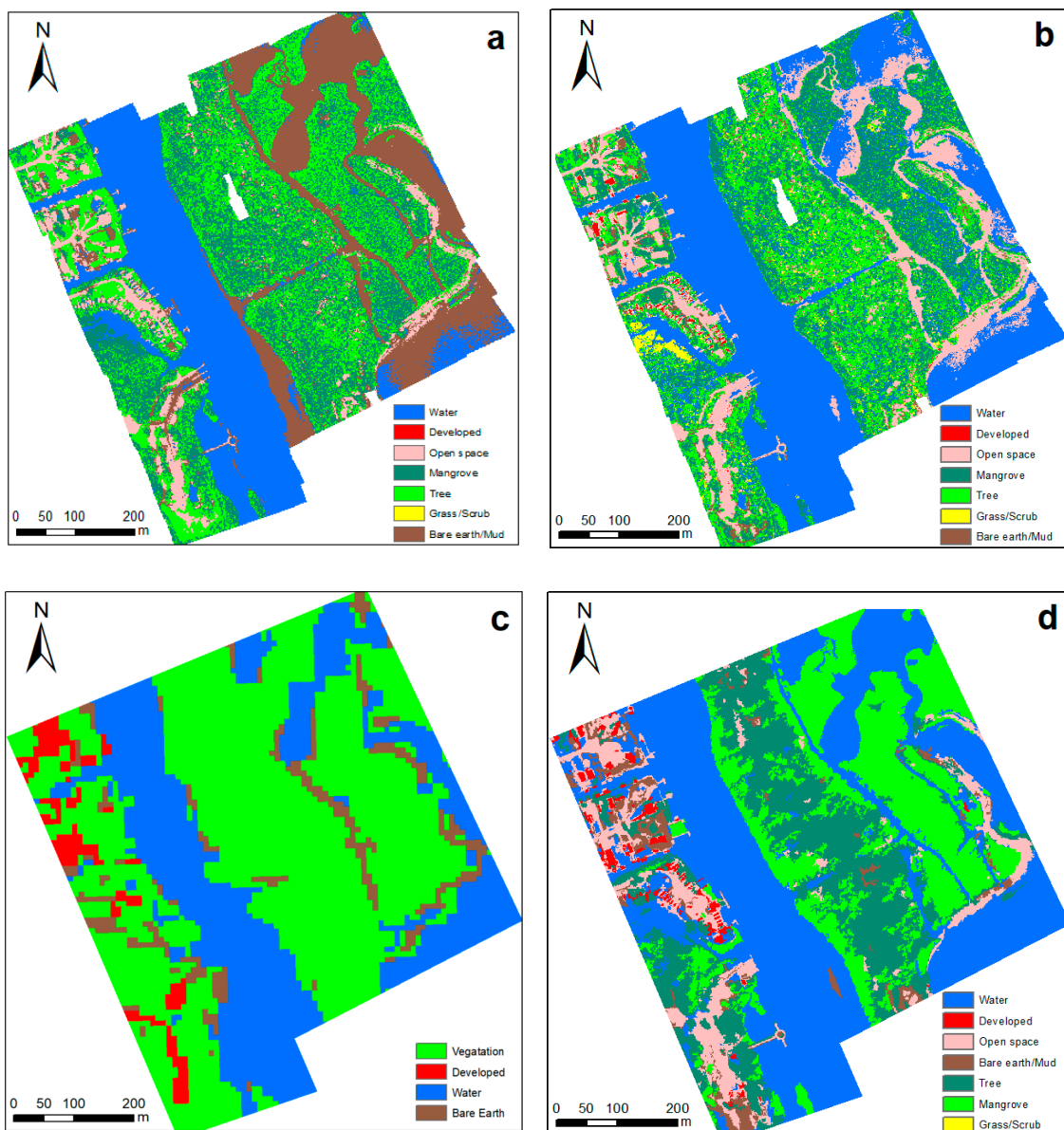


Figure 10. Comparison of classification results, (a) pixel-based classification on UAV data; (b) object-oriented classification on UAV data; (c) object-oriented classification on Sentinel-2 data; (d) object-oriented classification on aerial data.

Figure 10 shows the comparison of classification results of the UAV, satellite, and aerial data. Using the satellite classification method, the UAV data achieved higher accuracy and more detailed classification results (Figure 10b) than the satellite data (Figure 10c). For the satellite remote sensing classifications, only the major area of the vegetation coverage can be extracted from the image. There are few detailed variations inside of the lagoon area, and the mangrove forests cannot be distinguished from the adjacent root or scrub. The dense vegetation is mixed with all other vegetations to a similar homogeneous region. The shapes of residential areas and developed areas are not clear either. Roads, decks, and boundaries of the lagoon are much clearer than that shown under the Sentinel-2 classification results (Figure 10d).

4.4. Examining the Benefits of Finer Resolution Data

In addition to demonstrating the advantages of high spatial resolution UAV mapping and classification, we also aimed to examine the quantitative improvements of the UAV mapping compared

to conventional satellite remote sensing. To calculate how much improvement there was between these two types of mapping methods, we adopted a classification validation measurement of Kappa statistics [37,38]. The approach taken is based on Cohen's Kappa statistic, which is proposed as a standard meter for measuring the accuracy of all multi-valued classification problems [39]. Cohen's Kappa was first utilized as a measurement to estimate the degree of agreement or disagreement of two or more observers for the same phenomenon [40]. When comparing two or more digital classification results, the Kappa statistic is able to discriminate errors in terms of both quantity and location and to measure the overall accuracy of agreement between the classification and reference images. Its value ranges from 0 to 1, where 0 means no agreement and 1 means perfect agreement between the two classifications. In this research, we use the aerial imagery as reference to compare UAV mapping with conventional satellite remote sensing.

For validation, both the UAV classification and satellite remote sensing classification were compared with the aerial imagery using the K-fold cross-validation method. Two-thousand points were randomly selected to calculate the confusion matrix and Kappa value against the reference data, and we repeated the calculation 3 times. That is, we calculated the multiple confusion matrices based on various points selected, and the average Kappa value was used to compare the results. The minimum allowed distance between points was set to 10 m to ensure an even spatial distribution. To standardize for comparison purposes, the classification results from UAV and aerial mapping were merged into different types of vegetation classes in UAV and aerial mapping to a single class, so that they have the same class number for all types of data. That is, grass, trees, and mangroves are categorized as vegetation coverage, while open space and highly developed areas are categorized as developed area in the comparison of satellite classification results. When the UAV mapping products were compared with the aerial data, the 3-fold average value of the Kappa score was 0.713. Likewise, the 3-fold average value of the Kappa score for the satellite remote sensing mapping product was 0.538. Therefore, it can be noticed that compared with the reference data, UAV mapping classification results outperform the conventional satellite remote sensing in terms of a higher Kappa score (24.5% higher). In addition, Fleiss considers Kappa as excellent when more than 0.7; 0.40–0.7 as fair to good; and poor when Kappa is less than 0.4 [41]. Based on this study, the UAV mapping generates an excellent classification result against the reference data, with satellite remote sensing data only generating results in the “good” level.

5. Conclusion

Numerous research studies have discussed the advantages/disadvantages of different kinds of remote sensing approaches [6,42]. Traditional satellite remote sensing can retrieve historical data back to the 1960s with varied revisiting cycles. Although the data is convenient to obtain by researchers, the relatively coarse spatial resolution limits the application of satellite imagery in coastal monitoring and management. Aerial imagery provides very high spatial resolution, but it is cost prohibitive because of airplane and pilot costs. UAV/drone mapping techniques have developed in recent years as a cost-effective improvement to these two mapping methods. UAV imagery with its high spatial resolution, temporal flexibility, and ability to repeat photogrammetry in a short period affords a significant advancement on other remote sensing approaches, and UAV mapping can be widely used for coastal mapping, vegetation monitoring, and environmental management.

In this research, we implemented both multispectral and RGB UAV-collected images and SfM-MVS processing to examine a portion of Mosquito Lagoon along the central Atlantic coast of Florida. Ground Control Points were also collected in the field to support the stitching and geo-referencing of the drone images. High resolution multi-spectral mapping products at 0.25 m spatial resolution were generated to investigate the land cover classification results over the study region. Meanwhile, satellite remote sensing imagery (Sentinel-2) at 10 m spatial resolution was compared with the UAV mapping results. We calculated the well-established remote sensing index NDVI to illustrate the higher spatial details that can be extracted from the UAV mapping method. In comparison to coarse resolution satellite imagery, the UAV mapping method used in this study provided advanced information about the

physical conditions of the study area, an improved land feature delineation, and a more comprehensive understanding of the conditions of the mangroves.

Comparing the spatial resolution of the UAV mapping products and classification results, we examined whether the better-quality source data could provide results that would be more indicative of actual environmental management. Qualitatively, the multi-spectral UAV mapping provides a tremendous improvement of the spatial resolution, as well as much more detailed spatial information. Also, the NDVI map derived from UAV multi-spectral mapping is informative and with higher variance than the satellite imagery. Histogram comparison of the NDVI map demonstrated a more comprehensive multi-Gaussian distribution from the UAV mapping. Quantitatively, the kappa statistical score was calculated via the estimation of a confusion matrix, and a K-fold comparison was made between UAV classification and satellite classification against the reference data, respectively. The validation results show that UAV mapping classification results surpassed the conventional satellite remote sensing by 24.5% in terms of average Kappa score. The method presented in this paper quantitatively compares UAV mapping methods with conventional satellite imagery methods for coastal environments. This study not only demonstrates a methodology for multi-spectral drone coastal mapping with object-oriented classification but also provides a quantitative estimation of improvements of a UAV technique. It is our hope that the results of this study demonstrate the quantitative improvements of UAV imagery compared to conventional satellite imagery for image classification related to coastal environments and related management projects. Moreover, the application of multi-spectral UAV work presented in this study may be useful in other coastal areas of the world, especially areas with poor quality imagery.

Author Contributions: conceptualization, B.Y. and T.L.H.; methodology, B.Y. and T.L.H.; software, B.Y. and M.F.; validation, T.L.H. and H.T.; formal analysis, B.Y.; investigation, B.Y.; resources, B.Y. and T.L.H.; data curation, B.Y., H.T. and M.F.; writing—original draft preparation, B.Y.; writing—review and editing, T.L.H. and H.T.; visualization, B.Y.; supervision, T.L.H.; project administration, T.L.H.; funding acquisition, T.L.H.

Funding: This research was funded by the U.S. National Science Foundation under Grant No. 1829890 and the University of Central Florida Preeminent Postdoctoral Program.

Acknowledgments: This material is based upon work supported by the National Science Foundation. Thanks also to Tori-Gaye Atterbury, Hunter Searson, Amber Rutstein for their contributions collecting data on this project. This article is part of the broader research of Citizen Science GIS at University of Central Florida. We thank the editor and anonymous reviewers for their time and for improving the final article.

Conflicts of Interest: The authors declare no conflicts of interest.

References

1. Pujiono, E.; Kwak, D.-A.; Lee, W.-K.; Kim, S.-R.; Lee, J.Y.; Lee, S.-H.; Park, T.; Kim, M.-I. RGB-NDVI color composites for monitoring the change in mangrove area at the Maubesi Nature Reserve, Indonesia. *For. Sci. Technol.* **2013**, *9*, 171–179. [[CrossRef](#)]
2. Zhang, K.; Thapa, B.; Ross, M.; Gann, D. Remote sensing of seasonal changes and disturbances in mangrove forest: A case study from South Florida. *Ecosphere* **2016**, *7*, 1–23. [[CrossRef](#)]
3. Pu, R.; Bell, S. A protocol for improving mapping and assessing of seagrass abundance along the West Central Coast of Florida using Landsat TM and EO-1 ALI/Hyperion images. *ISPRS J. Photogramm. Remote Sens.* **2013**, *83*, 116–129. [[CrossRef](#)]
4. Tucker, C. Red and photographic infrared linear combinations for monitoring vegetation. *Remote Sens. Environ.* **1979**, *8*, 127–150. [[CrossRef](#)]
5. Kerr, J.T.; Ostrovsky, M. From space to species: Ecological applications for remote sensing. *Trends Ecol. Evolut.* **2003**, *18*, 299–305. [[CrossRef](#)]
6. Colomina, I.; Molina, P. Unmanned aerial systems for photogrammetry and remote sensing: A review. *ISPRS J. Photogramm. Remote Sens.* **2014**, *92*, 79–97. [[CrossRef](#)]
7. Wyngaard, J.; Barbieri, L.; Thomer, A.; Adams, J.; Sullivan, D.; Parr, C.; Raj Shrestha, S.; Crosby, C.; Klump, J.; Bell, T. Emergent Challenges for Science Suas Data Management: Fairness through Community Engagement and Best Practices Development. *Preprints* **2019**, 2019050274. [[CrossRef](#)]

8. Guo, M.; Li, J.; Sheng, C.; Xu, J.; Wu, L. A review of wetland remote sensing. *Sensors* **2017**, *17*, 777. [[CrossRef](#)]
9. Klemas, V.V. Coastal and environmental remote sensing from unmanned aerial vehicles: An overview. *J. Coast. Res.* **2015**, *315*, 1260–1267. [[CrossRef](#)]
10. Lottes, P.; Khanna, R.; Pfeifer, J.; Siegwart, R.; Stachniss, C. UAV-based crop and weed classification for smart farming. In Proceedings of the 2017 IEEE International Conference on Robotics and Automation (ICRA), Singapore, 29 May–3 June 2017; IEEE: Piscataway, NJ, USA, 2017; pp. 3024–3031.
11. Cruzan, M.B.; Weinstein, B.G.; Grasty, M.R.; Kohn, B.F.; Hendrickson, E.C.; Arredondo, T.M.; Thompson, P.G. Small unmanned aerial vehicleS (micro-uavS, droneS) in plant ecology. *Appl. Plant Sci.* **2016**, *4*, 1600041. [[CrossRef](#)]
12. Mitchell, J.J.; Glenn, N.F.; Anderson, M.O.; Hruska, R.C.; Halford, A.; Baun, C.; Nydegger, N. Unmanned aerial vehicle (UAV) hyperspectral remote sensing for dryland vegetation monitoring. In Proceedings of the 2012 4th Workshop on Hyperspectral Image and Signal Processing (WHISPERS), 4–7 June 2012; IEEE: Shanghai, China, 2012; pp. 1–10.
13. Uto, K.; Seki, H.; Saito, G.; Kosugi, Y. Characterization of rice paddies by a UAV-Mounted miniature Hyperspectral sensor system. *IEEE J. Sel. Top. Appl. Earth Obs. Remote Sens.* **2013**, *6*, 851–860. [[CrossRef](#)]
14. Cao, J.; Leng, W.; Liu, K.; Liu, L.; He, Z.; Zhu, Y. Object-Based mangrove species classification using unmanned aerial vehicle hyperspectral images and digital surface models. *Remote Sens.* **2018**, *10*, 89. [[CrossRef](#)]
15. Berni, J.A.J.; Zarco-Tejada, P.J.; Suárez, L.; González-Dugo, V.; Fereres, E. Remote sensing of vegetation from UAV platforms using lightweight multispectral and thermal imaging sensors. *Int. Arch. Photogramm. Remote Sens. Spat. Inform. Sci.* **2009**, *38*, 6.
16. Zarco-Tejada, P.J.; González-Dugo, V.; Berni, J.A.J. Fluorescence, temperature and narrow-band indices acquired from a UAV platform for water stress detection using a micro-hyperspectral imager and a thermal camera. *Remote Sens. Environ.* **2012**, *117*, 322–337. [[CrossRef](#)]
17. Harvey, M.C.; Pearson, S.; Alexander, K.B.; Rowland, J.; White, P. Unmanned aerial vehicles (UAV) for cost effective aerial orthophotos and digital surface models (DSMs). In Proceedings of the 2014 New Zealand Geothermal Workshop, Auckland, New Zealand, 24–26 November 2014.
18. Rock, G.; Ries, J.; Udelhoven, T. Sensitivity analysis of UAV-photogrammetry for creating digital elevation models (DEM). In Proceedings of the Conference on Unmanned Aerial Vehicle in Geomatics, Zurich, Switzerland, 14–16 September 2011.
19. Uysal, M.; Toprak, A.; Polat, N. DEM generation with UAV Photogrammetry and accuracy analysis in Sahitler hill. *Measurement* **2015**, *73*, 539–543. [[CrossRef](#)]
20. Liu, H. Algorithmic foundation and software tools for extracting shoreline features from remote sensing imagery and LiDAR data. *J. Geogr. Inf. Syst.* **2011**, *03*, 99–119. [[CrossRef](#)]
21. Brockmeyer, R.; Rey, J.; Virnstein, R.; Gihnoe, R. Rehabilitation of impounded estuarine wetlands by hydrologic reconnection to the Indian River Lagoon, Florida (USA). *Wetl. Ecol. Manag.* **1996**, *4*, 93–109. [[CrossRef](#)]
22. Virnstein, R.W. Seagrass landscape diversity in the Indian River Lagoon, Florida: The importance of geographic scale and pattern. *Bull. Mar. Sci.* **1995**, *57*, 67–74.
23. Stroppiana, D.; Migliazzi, M.; Chiarabini, V.; Crema, A.; Musanti, M.; Franchino, C.; Villa, P. Rice yield estimation using multispectral data from UAV: A preliminary experiment in northern Italy. In Proceedings of the 2015 IEEE International Geoscience and Remote Sensing Symposium (IGARSS), 26–31 July 2015; IEEE: Milan, Italy, 2015; pp. 4664–4667.
24. Themistocleous, K. The use of UAV platforms for remote sensing applications: Case studies in Cyprus. In Proceedings of the Second International Conference on Remote Sensing and Geoinformation of the Environment (RSCy2014), 12 August 2014.
25. Xu, M.; Liu, H.; Beck, R.; Lekki, J.; Yang, B.; Shu, S.; Liu, Y.; Benko, T.; Anderson, R.; Tokars, R.; et al. Regionally and Locally Adaptive Models for Retrieving Chlorophyll-a Concentration in Inland Waters From Remotely Sensed Multispectral and Hyperspectral Imagery. *IEEE Trans. Geosci. Remote Sens.* **2019**, *57*, 4758–4774. [[CrossRef](#)]
26. Toming, K.; Kutser, T.; Laas, A.; Sepp, M.; Paavel, B.; Nõges, T. Undefined First experiences in mapping lake water quality parameters with Sentinel-2 MSI imagery. *Remote Sens.* **2016**, *8*, 640. [[CrossRef](#)]

27. Chen, J.; Zhu, W.; Tian, Y.Q.; Yu, Q.; Zheng, Y.; Huang, L. Remote estimation of colored dissolved organic matter and chlorophyll-a in Lake Huron using Sentinel-2 measurements. *J. Appl. Remote Sens.* **2017**, *11*, 1. [[CrossRef](#)]
28. Rouse, J.W., Jr.; Haas, R.H.; Schell, J.A.; Deering, D.W. *Monitoring the Vernal Advancement and Retrogradation (Green Wave Effect) of Natural Vegetation*; NASA: Washington, DC, USA, 27 May 1974.
29. Zhou, Y.; Michalak, A.M. Characterizing attribute distributions in water sediments by geostatistical downscaling. *Environ. Sci. Technol.* **2009**, *43*, 9267–9273. [[CrossRef](#)] [[PubMed](#)]
30. Jacquin, A.; Misakova, L.; Gay, M. A hybrid object-based classification approach for mapping urban sprawl in periurban environment. *Landscape Urb. Plan.* **2008**, *84*, 152–165. [[CrossRef](#)]
31. Li, C.; Wang, J.; Wang, L.; Hu, L.; Gong, P. Comparison of classification algorithms and training sample sizes in urban land classification with landsat thematic mapper imagery. *Remote Sens.* **2014**, *6*, 964–983. [[CrossRef](#)]
32. Benz, U.C.; Hofmann, P.; Willhauck, G.; Lingenfelder, I.; Heynen, M. Multi-resolution, object-oriented fuzzy analysis of remote sensing data for GIS-ready information. *ISPRS J. Photogramm. Remote Sens.* **2004**, *58*, 239–258. [[CrossRef](#)]
33. Liu, H.; Wang, L.; Sherman, D.; Gao, Y.; Wu, Q. An object-based conceptual framework and computational method for representing and analyzing coastal morphological changes. *Int. J. Geogr. Inf. Sci.* **2010**, *24*, 1015–1041. [[CrossRef](#)]
34. Zhang, Q.; Liu, C.; Zhang, G.; Zhou, A. Adaptive image segmentation by using mean-shift and evolutionary optimisation. *IET Image Process.* **2014**, *8*, 327–333.
35. Wang, R.; Wan, B.; Guo, Q.; Hu, M.; Zhou, S. Mapping regional urban extent using NPP-VIIRS DNB and MODIS NDVI data. *Remote Sens.* **2017**, *9*, 862. [[CrossRef](#)]
36. Makkeasorn, A.; Chang, N.-B.; Li, J. Seasonal change detection of riparian zones with remote sensing images and genetic programming in a semi-arid watershed. *J. Environ. Manag.* **2009**, *90*, 1069–1080. [[CrossRef](#)]
37. Stehman, S.V. Selecting and interpreting measures of thematic classification accuracy. *Remote Sens. Environ.* **1997**, *62*, 77–89. [[CrossRef](#)]
38. Pontius, R.G.; Cornell, J.D.; Hall, C.A. Modeling the spatial pattern of land-use change with GEOMOD2: Application and validation for Costa Rica. *Agric. Ecosyst. Environ.* **2001**, *85*, 191–203. [[CrossRef](#)]
39. Ben-David, A. Comparison of classification accuracy using Cohen's Weighted Kappa. *Expert Syst. Appl.* **2008**, *34*, 825–832. [[CrossRef](#)]
40. Cohen, J. A Coefficient of Agreement for Nominal Scales. *Educ. Psychol. Meas.* **1960**, *20*, 37–46. [[CrossRef](#)]
41. Fleiss, J.L.; Cohen, J.; Everitt, B.S. Large sample standard errors of kappa and weighted kappa. *Psychol. Bull.* **1969**, *72*, 323. [[CrossRef](#)]
42. McEvoy, J.F.; Hall, G.P.; McDonald, P.G. Evaluation of unmanned aerial vehicle shape, flight path and camera type for waterfowl surveys: Disturbance effects and species recognition. *PeerJ* **2016**, *4*, e1831. [[CrossRef](#)]



© 2019 by the authors. Licensee MDPI, Basel, Switzerland. This article is an open access article distributed under the terms and conditions of the Creative Commons Attribution (CC BY) license (<http://creativecommons.org/licenses/by/4.0/>).